

Initial Dislocation Structure and Dynamic Dislocation Multiplication In Mo Single Crystals

L. M. Hsiung and D. H. Lassila¹

Abstract: Initial dislocation structures in as-annealed high-purity Mo single crystals, and deformation substructures of the crystals compressed at room temperature under different strain rates have been examined and studied in order to elucidate the physical mechanisms of dislocation multiplication and motion in the early stages of plastic deformation. The initial dislocation density was measured to be in a range of $10^6 \sim 10^7 \text{ cm}^{-2}$. More importantly numerous grown-in superjogs were observed along screw dislocation lines. After testing in compression, dislocation density (mainly screw dislocations) increased to $10^7 \sim 10^8 \text{ cm}^{-2}$. Besides, the formation of dislocation dipoles (debris) due to the nonconservative motion of jogged screw dislocations was found to be dependent of the strain rates. While little dislocation dipoles (debris) were found in the crystal tested quasi-statically (10^{-3} s^{-1}), more cusps along screw dislocation lines and numerous dislocation dipoles (debris) were observed in the crystal compressed under the strain rate of 1 s^{-1} . Physical mechanisms for dislocation multiplication as well as dipole formation from jogged screw dislocations under different strain rate conditions are accordingly proposed and discussed.

1 Introduction

Since the initial discovery of dislocations in 1934 [Orowan (1934); Polanyi (1934); Taylor (1934)], it has been realized that crystal plasticity properties are derivable, at least in principle, from the aggregate behavior of dislocations. However, a quantitative connection between dislocation theory and the phenomenology of crystal plasticity is yet to be established owing to the immense computational complexity of the task for dealing with a large number of dislocations and the multi-

tude of their physical behaviors. Starting in the early 90's [Kubin et al. (1992)], the realization that bigger and faster computers may be used for crystal plasticity simulations has led to the development of a powerful computational methodology for dislocation dynamics (DD). The predictive power of the various DD implementations available today is based on their ability to incorporate, in a computationally tractable manner, multiple and complex mechanisms of dislocation behavior. While the current trend in DD simulations is to let dislocations behave most naturally [Rhee et al. (1998); Schwarz and Tersoff (1996)], computational limitations often dictate that simplified rules for dislocation unit processes to be adopted [Kubin et al. (1992)]. One of the key uncertainties in the DD simulations is how dislocations multiply and move during plastic deformation. To date, several dislocation multiplication mechanisms have been proposed in literature. Typically, dislocation multiplication is considered to take place when a dislocation attains a certain configuration. For example, the well-known Frank-Read (FR) source [Frank and Read (1950)] requires a configuration that both ends of a mobile dislocation segment be pinned (constrained) at two points as a result of either dislocation network or dislocation bend. However, because of an ill-defined nature of pinning points for dislocation multiplication, dislocation sources are usually introduced in the DD simulations in a presumption or an ad hoc manner by setting up a constrained dislocation configuration, which is most often unrealistic. For instance, the initial dislocation configuration for an FR multiplication source may be simply given as a dislocation segment linked between two pinning points with an arbitrarily given length, and dislocation multiplication may thus be mimic or simulated according to the FR multiplication mechanism.

In order to make the DD simulations for dislocation multiplication more realistic, there is a need to understand the correlation between initial dislocation structures (dislocation density, dislocation configuration, free dislocation link length, and grown-in jogs...) and dislocation mul-

¹ Lawrence Livermore National Laboratory
Chemistry and Materials Science Directorate
L-352, P.O. Box 808
Livermore, CA 94551-9900
hsiung1@llnl.gov

tiplication during plastic deformation. Accordingly, the main purpose of this investigation is to examine and compare the initial dislocation structures of annealed (high-purity) Mo crystals, and deformation substructures of slightly compressed Mo crystals in order to elucidate the underlying mechanisms of dislocation multiplication and motion during early stages of plastic deformation. Since numerous grown-in superjogs have been observed along dislocation lines within as-annealed Mo crystals, emphasis has been placed upon the strain-rate effect of kink-jog interactions on the dislocation multiplication and motion in the early stages of plastic deformation in Mo single crystals. A preliminary result is reported here.

2 Experimental

Since the Mo single crystals used for dislocation dynamics experiment must have high purity and low dislocation density in order to establish initial conditions for subsequent dislocation dynamics simulations, the high-purity Mo single crystals were fabricated using a standard electron-beam melting process by Accumet Materials Company, Ossining, NY. The interstitial impurities (ppm in weight) in the as-fabricated crystals are O: 25; N: < 10; H: < 5; C: < 10, respectively. Prior to compression test, the test samples were heat treated at 1500° C for 1 h, 1200° C for 1 h, and 1000° C for 1 h at a vacuum of 8×10^{-11} Torr. Testing of Mo single crystals involves compressing the test samples between two platen surfaces under precise conditions. To measure shear strain during compression, a 3-element rosette gage was bonded in the gage section on each side of the sample. Compression tests were performed on test samples with [118] and $[\bar{2} 9 20]$ compression axes. These two orientations were originally chosen to investigate deformation behavior associated with the $(\bar{1}\bar{1}2)[111]$ and $(\bar{1}01)[111]$ slip systems, respectively. The samples were compressed at a normal strain rate of 10^{-3} s^{-1} for the [118]-oriented sample, and 1 s^{-1} for the $[\bar{2} 9 20]$ -oriented sample, and both samples were compressed to a value of $\sim 1\%$ axial strain. TEM foils were sliced from the gage section of the tested piece with the foil sliced parallel to the $(\bar{1}\bar{1}2)$ plane from [118]-oriented sample, and the $(\bar{1}01)$ plane for the $[\bar{2} 9 20]$ -oriented sample. TEM specimens were finally prepared by a standard twinjet electropolishing technique in a solution of 75 vol.% ethanol and 25 vol.% sulfuric acid at $\sim 25 \text{ V}$ and -10° C .

3 Results and Discussion

3.1 Initial dislocation structures

Figure 1 shows the initial dislocation structures observed from the [011]-, $[0\bar{1}1]$ -, and [100]-sliced foils (as illustrated here on the three surfaces of a box). The dislocation density (ρ) of an as-annealed Mo single crystal is estimated to be on the order of $10^6 \sim 10^7 \text{ cm}^{-2}$. According to the Frank-Read dislocation multiplication mechanism [Frank and Read (1950)], dislocation can multiply by repeatedly bowing out a free segment of dislocation line lying in a slip plane, and the shear stress (τ) required to bow out a line segment (l) is given as: $\tau \approx \mu b/l$. Thus, there may exist a critical length ($l^* \approx \mu b/\tau_a$) of free segment for a given applied shear stress (τ_a). Any length of free segment l which is smaller than l^* will be permanently immobile, while length of segment greater than l^* are potentially mobile. Accordingly, an investigation of the relative density (ρ_m/ρ) of mobile dislocation in slip plane is important for studying the yielding behavior of a crystal. An investigation made on this aspect of dislocation configuration is shown in Fig. 2. Here, “in-plane” $\frac{1}{2}[111]$ near-screw dislocations with a finite segment length in the $\{\bar{1}01\}$ planes are shown in Fig. 2(a). However, there is an uncertainty whether the observed segment is truly a free dislocation segment without any other pinning points such as short jog segments associated with the dislocation line. In other words, there is a difficulty to define free segment length by viewing dislocation from this orientation since it is infeasible to locate the pinning points formed by jog segments along the dislocation line. In fact, the dislocation segment length viewed from the $\{\bar{1}01\}$ -sliced foils may be a measure of the line waviness along the foil normal (or line waviness through thickness). That is, the finite dislocation segment shown in Fig. 2(a) suggests that the dislocation line in the annealed crystals is actually lying across many planes instead of sitting in single crystallographic plane as one usually anticipates. This implies that the initial dislocation structure may contain grown-in jogs of like-sign along a dislocation line and causing the dislocation line to terminate at the free surfaces of thin foil as schematically illustrated in Fig. 2(b).

In fact, the finite length of dislocation segment viewing from the $\{\bar{1}01\}$ -sliced foils may be a measure of the line waviness along the foil normal. This can be visualized readily from a cross-sectional view of $\frac{1}{2}[\bar{1}\bar{1}1]$ screw dis-

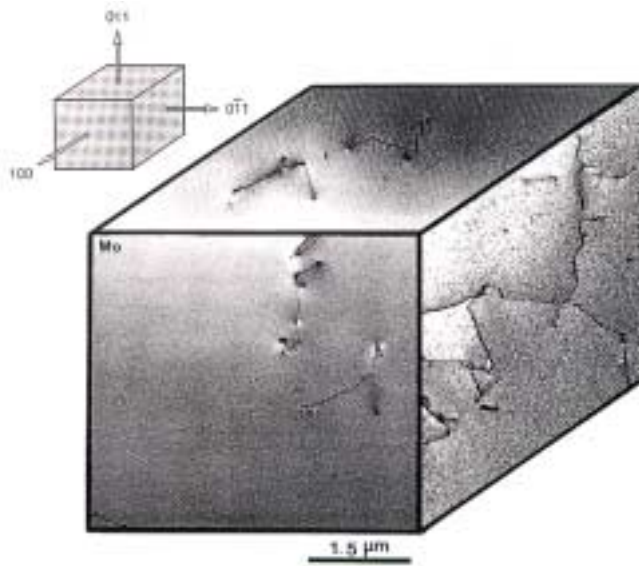


Figure 1 : Initial dislocation structure of an as annealed Mo single crystal.

location shown in Fig. 3(a), in which the screw dislocation in the (011) plane was observed from the foil sliced parallel to the $(0\bar{1}1)$ plane. Here, the existence of many long superjogs (50 ~100 nm in height) along the $\frac{1}{2} [\bar{1}11]$ screw dislocation line can be seen. In addition, the dislocation line is found to skew away from the $[\bar{1}11]$ direction revealing that the dislocation line is also associated with many short superjogs [jog height (d) < 1 nm] or elementary jogs [jog height = interplanar spacing of $(\bar{1}21)$ plane = 0.135 nm]. Noted that the height of short superjog or elementary jog is too short to be resolvable using TEM imaging techniques. This examination suggests that the short dislocation segments appeared in the $\{\bar{1}01\}$ -sliced foils is attributed to the formation of jogs along a screw dislocation line which causes it to lie across many $\{\bar{1}01\}$ planes instead of one. Consequently, screw dislocation lines are chopped into short segments in a $\{\bar{1}01\}$ -sliced TEM foils. Similarly, jogged $\frac{1}{2} [111]$ and $\frac{1}{2} [1\bar{1}\bar{1}]$ screw dislocations were also observed. A jogged $\frac{1}{2} [1\bar{1}\bar{1}]$ screw dislocation viewing from the $[0\bar{1}1]$ direction is shown in Fig. 3(b). Here, many large superjogs (50 ~100 nm in height) can be readily seen along the dislocation line. Also notice that the lengths of each free segment linked between two superjogs are unequal.

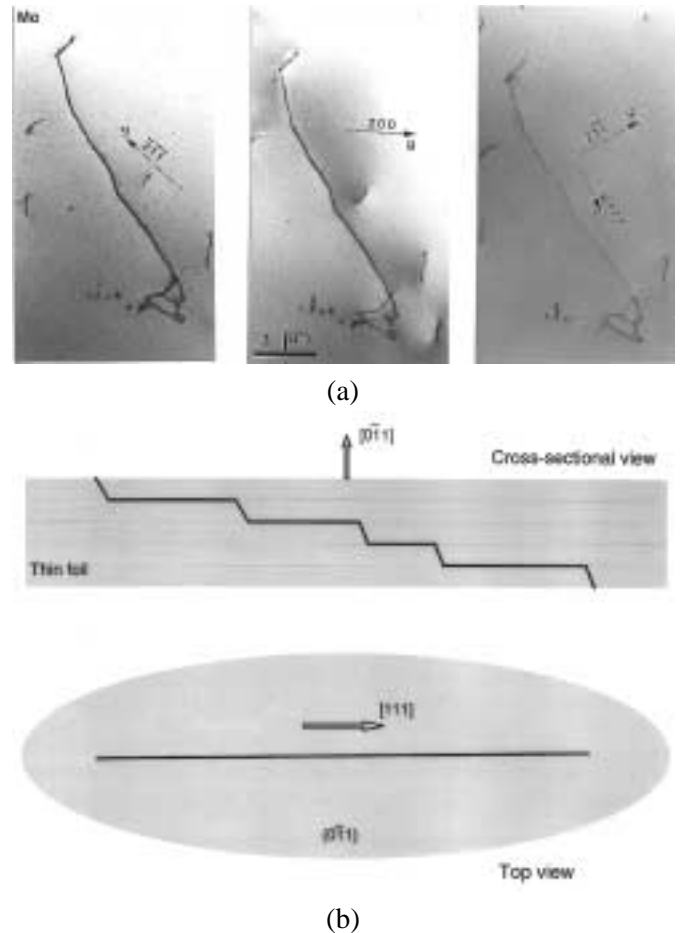
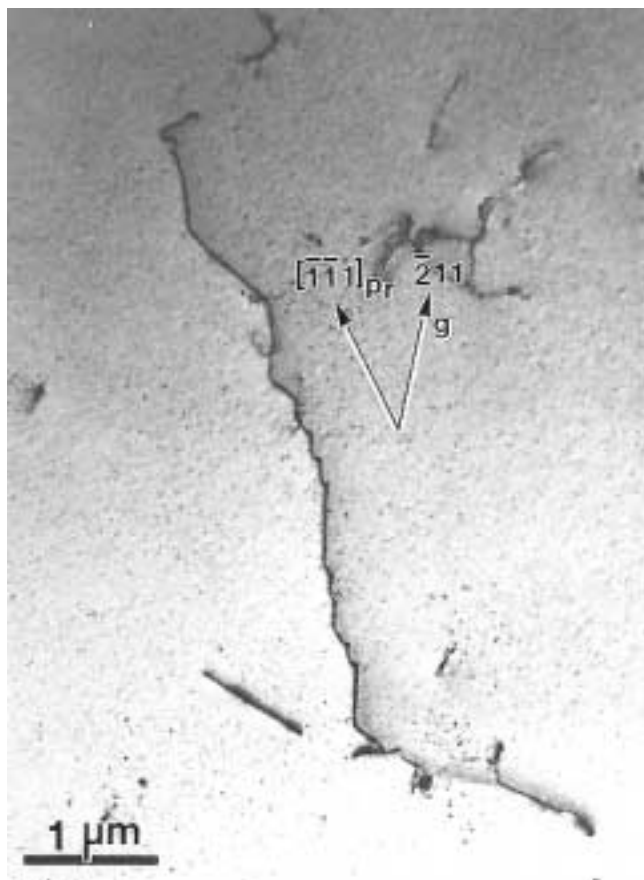
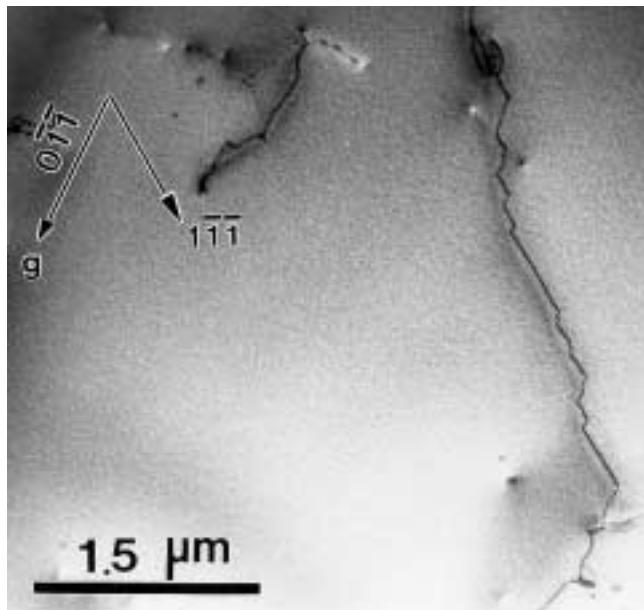


Figure 2 : (a) A $\mathbf{g} \cdot \mathbf{b}$ analysis for a $\pm \frac{1}{2} [111]$ screw dislocation formed in $(0\bar{1}1)$ -sliced Mo. (b) Schematic illustrations of cross-sectional and top views of a jogged screw dislocation line within a foil sliced parallel to the slip plane, in which the dislocation line terminates at the free surfaces of thin foil.



(a)



(b)

Figure 3 : TEM images showing (a) a jogged $\frac{1}{2}[\bar{1}\bar{1}1]$ screw dislocation and (b) a jogged $\frac{1}{2}[1\bar{1}\bar{1}]$ screw dislocation in as-annealed Mo; viewing direction: $[0\bar{1}\bar{1}]$.

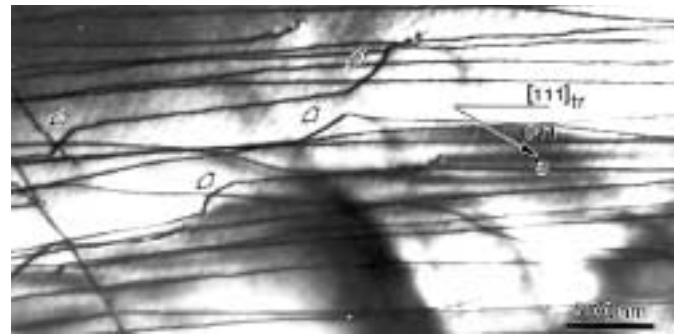


Figure 4 : TEM images showing $\frac{1}{2}[111]$ screw dislocations associated with superjogs (indicated by arrows) in a crystal compressed for 1% (strain rate: 10^{-3} s^{-1}), viewing direction: $[1\bar{1}\bar{1}]$.

3.2 Deformation substructures

Typical deformation substructures of Mo single crystals compressed for 1% under strain-rate of 10^{-3} s^{-1} and 1 s^{-1} are shown in Figs. 4(a) and 4(b), respectively. The dislocation density increases about two orders of magnitude to a range of $10^8 \sim 10^9 \text{ cm}^{-2}$. Notice in Fig. 4(a) that many superjogs (marked by arrows) can be seen along screw dislocation lines, and the average jog height, and free segments between superjogs were found to increase significantly as compared to those observed in as-annealed samples (Fig. 3). In general, the screw dislocation lines become straighter and longer comparing to those in as-annealed crystals. However, the formation of dislocation dipoles (debris) as a result of the nonconservative motion of jogged screw dislocations is dependent of the strain rates. While little dislocation dipole (debris) were found in the crystal tested quasi-statically (10^{-3} s^{-1}), more cusps along screw dislocation lines and many dislocation dipoles (debris) were observed in the crystal compressed under the strain rate of 1 s^{-1} as shown in Fig. 4(b).

3.3 Proposed mechanisms for dislocation multiplication and motion

Based upon the results of TEM observations shown above, mechanisms of dislocation multiplication and motion during the early stages of plastic deformation in Mo single crystals under different strain-rate conditions are proposed below. When deformed under a quasi-static condition, the dislocation multiplication is illustrated in Fig. 6. Here, screw dislocation segments (pinned by su-

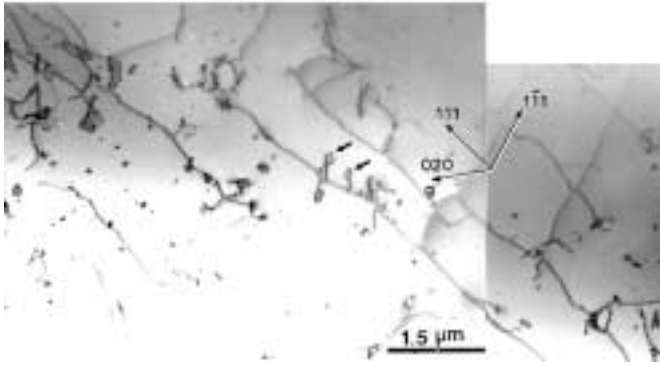


Figure 5 : TEM images showing (a) $\frac{1}{2}[111]$ screw dislocations associated with dislocation dipoles (indicated by arrows) and many dislocation debris in a crystal compressed for 1% (strain rate: 1 s^{-1}).

perjogs) bow out between the superjogs under an applied shear stress (τ) to a certain curvature, yet they are immobile since the initial length (l_o) of each free segment is smaller than a critical length ($l^* \approx \mu b/\tau$) as defined earlier. Beside the force exerted on dislocation segments by the applied shear stress, each superjog is subjected to a net force (F_x) parallel to the Burgers vector due to the bowing of unevenly spaced link segments between jogs under small strains, which is schematically illustrated in Fig. 6(d). The magnitude of net force can be expressed as:

$$F_x = \Gamma \cos \phi_2 - \cos \phi_1,$$

where $\phi = \sigma b l / 2\Gamma$ and Γ is the line tension. Applying Taylor expansion to $\cos \phi$ thus

$$F_x \approx \frac{b^2 \sigma^2}{8\Gamma} (l_1^2 - l_2^2).$$

The force causes large loop to grow at the expense of neighboring short loop by drifting the jog at P. The jog drifting velocity (v_j) can be related to its mobility (D_j/kT) according to the Einstein mobility relation [Hirth and Lothe (1981); Einstein (1926)]:

$$v_j = \frac{D_j}{kT} F_x$$

where D_j is the jog diffusivity. That is, each jog in Fig. 6(b) moves in such a direction so that the shorter segments (\overline{CD} and \overline{EF}) become still shorter and the longer segments (\overline{AB} and \overline{GH}) are expanded [Weertman and

Shahinian (1957)]. The jogs of like-sign tend to coalesce in order to reduced line energy and resulting in the increase of jog height [Louat and Johnson (1962)]. Consequently, the stress-induced jog pileup and coalescence renders an increase of both segment length and jog height.

Applied shear stress eventually begins to push each line segment between jogs [Fig. 6 (c)] to precede dislocation multiplication when the length (l) of line segments (\overline{IJ} and \overline{KL}) and height (d) of superjog (\overline{JK}) are greater than critical values defined as following.

$$L > l^* \approx \mu b/\tau, \text{ and}$$

$$d > d_c \approx \mu b/8\pi(1 - \nu)\tau.$$

Here, a mutual attraction force between adjacent bowing edge segments of opposite signs can define d_c . That is, the originally immobile screw dislocations become multiple sources for dislocation multiplication as a result of the process of jog migration and coalescence. This “dynamic” dislocation multiplication source is suggested to be crucial for the dislocation multiplication in the early stage of plastic deformation in Mo.

When deformed under a high strain-rate condition, the nucleation and migration of double kinks on screw dislocations become more rapidly according to the following equation [8]:

$$v_k = \frac{\sigma b L D_k}{kT} \exp\left[-\frac{2W_k}{kT}\right]$$

where, v_k is the migration velocity of double kinks, L the length of free segment, D_k/kT the kink mobility, D_k the kink diffusivity, W_k the formation energy for double kinks, which is considered to be a function of stress, i.e. it decreases with increasing applied stress. Accordingly, the rapid increase of stress on a link segment causes the double-kinks to pileup at the ends of the segment as shown in Fig. 7 (a). This in turn causes the angle θ to increase rapidly to approach 90° , which vanishes the net force on a superjog and thus retards the process for migration and coalescence of superjogs. Under this circumstance, long superjogs may still have sufficiently large jog-height to satisfy the condition for operating the “dynamic” multiplication source. Superjogs of relatively small height, on the other hand, will be unable to meet

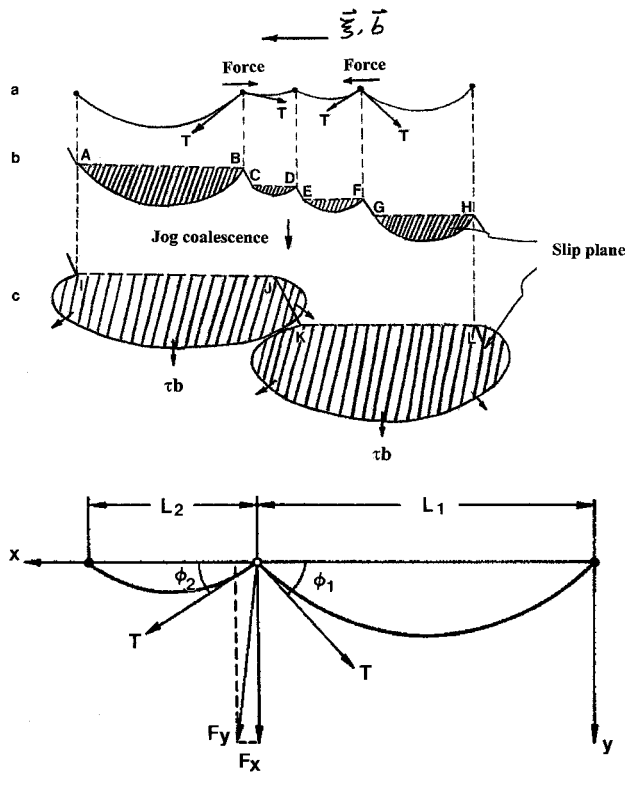


Figure 6 : Schematic illustrations of dislocation multiplication from a jogged screw dislocation. (a) A top view showing dislocation segments pinned by superjogs bowing under stress to a curvature, net forces are generated on jogs due to unbalanced line-tension partials acting on the free segments of unequal lengths. (b) A tilt view of (a) shows the initial heights of like-sign superjogs. (c) Both segment length and jog height increase due to stress-induced jog coalescence. As a result, two multiplication sources are generated at segments \overline{IJ} and \overline{KL} . (d) The resolved forces F_x and F_y acting on the jog (pinning point) caused by link segments of unequal lengths, L_1 and L_2 bowing under low strains.

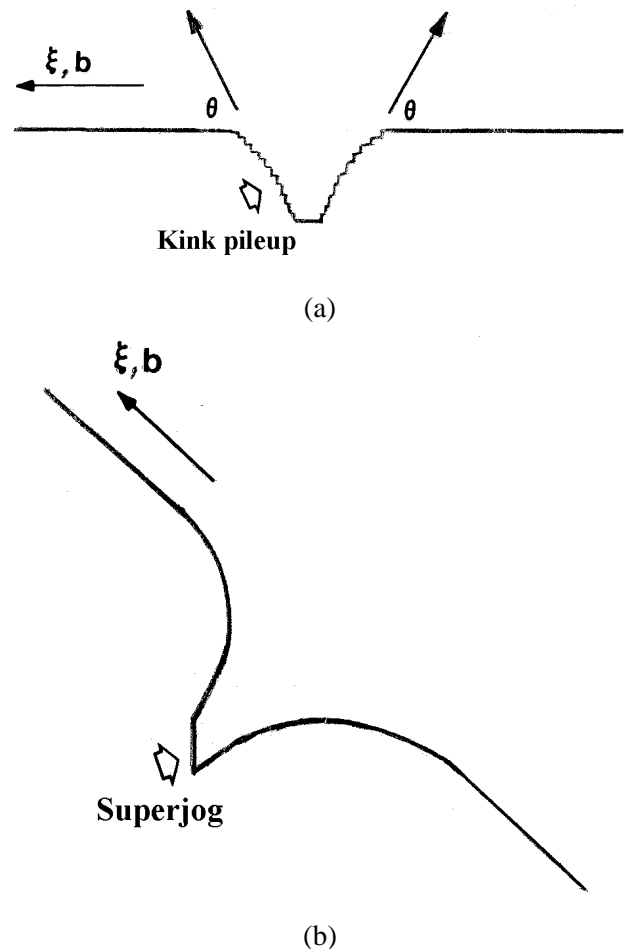


Figure 7 : Fig. 7. Schematic illustrations showing (a) the formation of superkinks as a result of the pileup of kinks at superjog, and (b) an edge dipole drawn out from a jogged screw dislocation

the condition for multiplication, and the gliding (jogged) screw dislocation will eventually draw out a dislocation dipole as shown in Fig. 7 (b), in which a dislocation dipole consists of two parallel dislocation segments of opposite signs, and are separated from each other by a short distance depending on the jog height (d).

4 Conclusions

Initial dislocation structures in as-annealed high-purity Mo single crystals, and deformation substructures of the crystals compressed at room temperature under different strain rates (10^{-3} s^{-1} and 1 s^{-1}) have been examined and studied in order to elucidate the physical mechanisms of dislocation multiplication and motion for dislocation dy-

namics simulations. It is suggested that the jogged screw dislocations can act as predominant sources for either dislocation multiplication or dipole (debris) formation depending on applied strain rates. When compressed under a quasi-static condition, both the superjog height and length of link segment (between superjogs) can increase by stress-induced jog migration and coalescence, which presumably takes place via the lateral migration (drift) of superjogs driven by unbalanced line-tension partials acting on link segments of unequal lengths. Applied stress begins to push each link segment to precede dislocation multiplication when link length and jog height become greater than critical values. When compressed under a high strain-rate condition, the rapid increase of stress on a link segment causes the nucleation and migration of more double-kinks to pileup at the ends of the segment, which in turn retards the process of jog migration and coalescence. Dislocation dipoles (debris) start to generate as a result of the nonconservative motion of jogged dislocations in which jog heights remain small.

Acknowledgement: This work was performed under the auspices of the U.S. Department of Energy by the University of California, Lawrence Livermore National Laboratory under contract No. W-7405-Eng-48. The authors would like to thank Dr. V. V. Bulatov for providing information regarding Dislocation Dynamics Simulations.

Reference

- Einstein A.** (1926): “*Investigations on the Theory of Brownian Movement*,” Methuen, London, pp. 9
- Frank F. C., Read W. T.** (1950): “*Symposium on Plastic Deformation of Crystalline Solids*,” Carnegie Institute of Technology, Pittsburgh, pp. 44
- Hirth J. P., Lothe J.** (1981): “*Theory of Dislocations*”, 2nd ed., J. Wiley, New York.
- Kubin L.P., Canova G., Condat M., Devincere B., Pontikis V., Brechet Y.** (1992): *Solid State Phenom*, **23-24**, pp. 455
- Louat N., Johnson C. A.** (1962): *Phil. Mag.*, **7**, pp. 2051
- Orowan E.** (1934): *Z. Phys.*, **89**, pp. 604
- Polanyi M.** (1934): *Z. Phys.*, **89**, pp. 660
- Rhee M., Zbib H.M., Hirth J.P., Huang H., Diaz de la Rubia T.** (1998): *Modeling Simul. Mater. Sci. Eng.*, **6** (1998), pp. 467
- Schwarz K.W., Tersoff J.** (1996): *Appl. Phys. Lett.*, **69** (1996), pp. 1220
- Taylor G.I.** (1943): *Proc. Roy. Soc, London* , **A145**, pp. 362
- Weertman J., Shahinian, P.** (1957): *Trans. A.I.M.E.*, **209**, pp. 1298

